Efficient iterative methods for multi-frequency wave propagation problems: A comparison study

Manuel Baumann and Martin B. van Gijzen

Delft University of Technology, Delft, The Netherlands
{m.m.baumann,m.b.vangijzen}@tudelft.nl

Abstract

In this paper we present a comparison study for three different iterative Krylov methods that we have recently developed for the simultaneous numerical solution of wave propagation problems at multiple frequencies. The three approaches have in common that they require the application of a single shift-and-invert preconditioner at a suitable *seed* frequency. The focus of the present work, however, lies on the performance of the respective iterative method. We conclude with numerical examples that provide guidance concerning the suitability of the three methods.

Keywords: Time-harmonic elastic wave equation, global GMRES, nested multi-shift GMRES, shifted polynomial preconditioners

1 Introduction

After spatial discretization, for instance using the finite element method [5] with N degrees of freedom, the time-harmonic wave equation has the form,

$$(K + i\omega_k C - \omega_k^2 M)\mathbf{x}_k = \mathbf{b}, \quad \omega_k := 2\pi f_k, \quad k = 1, ..., n_\omega, \tag{1}$$

with stiffness matrix K, mass matrix M, and C consisting of non-trivial boundary conditions [2]. Note that (1) yields a sequence of n_ω linear systems of equations. One way to solve the systems (1) simultaneously is to define the block matrix of unknowns, $\mathbf{X} := [\mathbf{x}_1, ..., \mathbf{x}_{n_\omega}] \in \mathbb{C}^{N \times n_\omega}$, and note that (1) can be rewritten as,

$$\mathcal{A}(\mathbf{X}) := K\mathbf{X} + iC\mathbf{X}\Omega - M\mathbf{X}\Omega^2 = B, \quad \text{with } \Omega := \text{diag}(\omega_1, ..., \omega_{n_\omega}) \text{ and } B := \mathbf{b}\mathbf{1}^\mathsf{T}. \tag{2}$$

The matrix equation (2) can then be solved using a global Krylov method. A second approach is a linearization [18] of the form,

$$\left(\begin{bmatrix} iC & K \\ I & 0 \end{bmatrix} - \omega_k \begin{bmatrix} M & 0 \\ 0 & I \end{bmatrix} \right) \begin{bmatrix} \omega_k \mathbf{x}_k \\ \mathbf{x}_k \end{bmatrix} = \begin{bmatrix} \mathbf{b} \\ \mathbf{0} \end{bmatrix}, \quad k = 1, ..., n_\omega, \tag{3}$$

where the angular frequencies $\omega_1, ..., \omega_{n_\omega}$ appear as a (linear) shift. For short-hand notation, we define the block matrices,

$$\mathcal{K} := \begin{bmatrix} iC & K \\ I & 0 \end{bmatrix} \in \mathbb{C}^{2N \times 2N} \quad \text{and} \quad \mathcal{M} := \begin{bmatrix} M & 0 \\ 0 & I \end{bmatrix} \in \mathbb{C}^{2N \times 2N},$$

and write (3) as $(\mathcal{K} - \omega_k \mathcal{M})\mathbf{x}_k = \mathbf{b},$ for $k = 1, ..., n_\omega$. We will consider the case $C \equiv 0$ independently. The matrix equation (2) then reduces to two terms, and we can identify $\mathcal{K} = K$ as well as $\mathcal{M} = M$ and avoid doubling of dimensions in (3). In this paper, we review and compare the following recently developed algorithms:

- Global GMRES [12] for the matrix equation approach [5] (cf. Algorithm 1),

- Polynomial preconditioners [1, 7] for multi-shift GMRES (cf. Algorithm 2),

- Nested multi-shift FOM-FGMRES as presented in [6] (cf. Algorithm 3-4).

This list does not consider a comparison with the algorithms suggested by [4, 16] and by [19, 20]. Moreover, we restrict ourselves to GMRES-variants of the respective methods, and refer to [3] for global IDR(s) and [6] for the more memory-efficient combination nested IDR-QMRIDR(s). In [1] a polynomial preconditioner is used within multi-shift BiCG. The derivations in Section 2 emphasize that the cost-per-iteration of each proposed algorithm is comparable. In Section 3, we evaluate the three approaches for a numerical benchmark problem of the discretized time-harmonic elastic wave equation.

2 Iterative Krylov methods for multi-frequency wave propagation problems

The review of the subsequent algorithms is based on our works [5, 6, 7].

2.1 Preconditioned matrix equation approach

The matrix equation (2) with right preconditioning reads,

$$\mathcal{A}(P(\tau)^{-1}\mathbf{Y}) = B, \quad \mathbf{X} = P(\tau)^{-1}\mathbf{Y}, \quad \text{where } P(\tau) := (K + i\tau C - \tau^2 M)^{-1}, \qquad (4)$$

and $\mathcal{A}(\cdot)$ as in (2). A similar reformulation has been suggested in [19]. We note that, for instance, the preconditioner $P(\tau)$ can be applied inexactly using an incomplete LU factorization. The (possibly complex) parameter τ is called the *seed* frequency. In Algorithm 1, we state the global GMRES method [12]. Note that in the block Arnoldi method the trace inner product is used, and norms are replaced by the Frobenius norm $\|\cdot\|_{\mathsf{F}}$ for block matrices. After m iterations, an approximate solution to (2) in the block Krylov subspace $\mathcal{K}_m(\mathcal{A}P(\tau)^{-1}, B)$ is obtained.

2.2 Preconditioners for shifted linear systems

The methods presented in this section are both two-level preconditioning approaches. As a first-level preconditioner, a shift-and-invert preconditioner of the form,

$$\mathcal{P}(\tau)^{-1} = (\mathcal{K} - \tau\mathcal{M})^{-1} = \left(\begin{bmatrix} iC & K \\ I & 0 \end{bmatrix} - \tau \begin{bmatrix} M & 0 \\ 0 & I \end{bmatrix} \right)^{-1}$$

$$= \begin{bmatrix} I & \tau I \\ 0 & I \end{bmatrix} \begin{bmatrix} I & 0 \\ 0 & (K + i\tau C - \tau^2 M)^{-1} \end{bmatrix} \begin{bmatrix} 0 & I \\ I & -iC + \tau M \end{bmatrix}, \qquad (5)$$

Algorithm 1 Right-preconditioned global GMRES for the matrix equation (2), cf. [12]

1: Set $R_0 = B$, $V_1 = R_0/\|R_0\|_\mathsf{F}$ $\qquad\qquad\qquad\qquad$ ▷ Initialization (when $X_0 = 0$)
2: **for** $j = 1$ to m **do**
3: $\qquad$ Apply $W = \mathcal{A}(P(\tau)^{-1}V_j)$ $\qquad\qquad\qquad$ ▷ Preconditioner might be inexact
4: $\qquad$ **for** $i = 1$ to j **do** $\qquad\qquad\qquad\qquad\qquad\qquad$ ▷ Block-Arnoldi method
5: $\qquad\qquad$ $h_{i,j} = \mathrm{tr}(W^\mathsf{H}V_i)$
6: $\qquad\qquad$ $W = W - h_{i,j}V_i$
7: $\qquad$ **end for**
8: $\qquad$ Set $h_{j+1,j} = \|W\|_\mathsf{F}$ and $V_{j+1} = W/h_{j+1,j}$
9: **end for**
10: Set $\underline{\mathrm{H}}_m = [h_{i,j}]_{i=1,...,m}^{j=1,...,m+1}$ and $\mathbf{V}_m = [V_1, ..., V_m]$ $\qquad$ ▷ $\mathbf{V}_m$ is basis of block Krylov space
11: Solve $\mathbf{y}_m = \mathrm{argmin}_\mathbf{y} \|\underline{\mathrm{H}}_m\mathbf{y} - \|B\|_\mathsf{F}\mathbf{e}_1\|_2$
12: Compute $\mathbf{X}_m = P(\tau)^{-1}(\mathbf{V}_m * \mathbf{y}_m)$ $\qquad\qquad\qquad$ ▷ '*' denotes the star product

---

is applied. Based on the decomposition (5) we note that $P(\tau)^{-1} = (K + i\tau C - \tau^2 M)^{-1}$ as defined in (4) is the main computational work and, hence, the work-per-iteration is comparable to Algorithm 1. For the block systems (3), the following equivalence holds,

$$(\mathcal{K} - \omega_k\mathcal{M})\mathcal{P}_k^{-1}\mathbf{y}_k = \mathbf{b} \quad \Leftrightarrow \quad (\mathcal{K}\mathcal{P}(\tau)^{-1} - \eta_k I)\mathbf{y}_k = \mathbf{b}, \tag{6}$$

where $\eta_k := \omega_k/(\omega_k - \tau)$, and $\mathcal{P}_k^{-1} := (1 - \eta_k)\mathcal{P}(\tau)^{-1} = (1 - \eta_k)(\mathcal{K} - \tau\mathcal{M})^{-1}$. Note that the latter is a preconditioned shifted linear system with (complex) shifts η_k and system matrix $\mathcal{C} := \mathcal{K}\mathcal{P}(\tau)^{-1} = \mathcal{K}(\mathcal{K} - \tau\mathcal{M})^{-1}$. Due to the equivalence in (6), the preconditioner (5) needs to be applied exactly.

2.2.1 Optimal polynomial preconditioners

After applying the shift-and-invert preconditioner (5) to (3), we remain with solving,

$$(\mathcal{C} - \eta_k I)\mathbf{y}_k = \mathbf{b}, \quad \mathbf{x}_k = \mathcal{P}_k^{-1}\mathbf{y}_k, \quad k = 1, ..., n_\omega, \tag{7}$$

where $\mathcal{C} = \mathcal{K}\mathcal{P}(\tau)^{-1}$, and with (complex) shifts $\eta_k = \omega_k/(\omega_k - \tau)$. Efficient algorithms for shifted systems (7) rely on the shift-invariance property, $\mathcal{K}_m(\mathcal{C}, \mathbf{b}) \equiv \mathcal{K}_m(\mathcal{C} - \eta I, \mathbf{b})$, for any shift $\eta \in \mathbb{C}$ when the base vector is at least collinear; cf. [11, 17]. The (preconditioned) spectrum of $\mathcal{C}$ is known to be enclosed by a circle of radius R and center c [7, 21]. Therefore, the Neumann preconditioner [15, Chapter 12.3] of degree n,

$$\mathcal{C}^{-1} \approx \sum_{i=0}^{n}(I - \xi\mathcal{C})^i =: p_n(\mathcal{C}), \quad \text{with } \xi = \frac{1}{c} = -\frac{\tau - \bar{\tau}}{\bar{\tau}}, \tag{8}$$

has optimal spectral radius. The polynomial preconditioner (8) can also be represented as $p_n(\mathcal{C}) = \sum_{i=0}^{n}\alpha_i\mathcal{C}^i$. Shift-invariance can be preserved if the following holds,

$$(\mathcal{C} - \eta_k I)p_{n,k}(\mathcal{C}) = \mathcal{C}p_n(\mathcal{C}) - \tilde{\eta}_k I, \tag{9}$$

where $p_{n,k}(\mathcal{C}) = \sum_{i=0}^{n}\alpha_{i,k}\mathcal{C}^i$ is a polynomial preconditioner for $(\mathcal{C} - \eta_k I)$. Substitution yields,

$$\sum_{i=0}^{n}\alpha_{i,k}\mathcal{C}^{i+1} - \sum_{i=0}^{n}\eta_k\alpha_{i,k}\mathcal{C}^i - \sum_{i=0}^{n}\alpha_i\mathcal{C}^{i+1} + \tilde{\eta}_k I = 0. \tag{10}$$

The latter (10) is a difference equation and can be solved in closed form [1]:

$$\alpha_{n,k} = \alpha_n \tag{11a}$$

$$\alpha_{i-1,k} = \alpha_{i-1} + \eta_k \alpha_{i,k}, \quad \text{for } i = n, ..., 1 \tag{11b}$$

$$\tilde{\eta}_k = \eta_k \alpha_{0,k} \tag{11c}$$

Algorithm 2 Multi-shift GMRES with polynomial preconditioner for (9), cf. [1, 7]

1: Set $\mathbf{r}_0 = \mathbf{b}$, $\mathbf{v}_1 = \mathbf{r}_0/\|\mathbf{r}_0\|$ ▷ Initialization
2: **for** $j = 1$ to m **do**
3:     Apply $\mathbf{w} = \mathcal{C}p_n(\mathcal{C})\mathbf{v}_j$ ▷ Polynomial preconditioner (8) of degree n
4:     **for** $i = 1$ to j **do**   ▷ Arnoldi method
5:         $h_{i,j} = \mathbf{w}^\mathsf{H}\mathbf{v}_i$
6:         $\mathbf{w} = \mathbf{w} - h_{i,j}\mathbf{v}_i$
7:     **end for**
8:     Set $h_{j+1,j} = \|\mathbf{w}\|$ and $\mathbf{v}_{j+1} = \mathbf{w}/h_{j+1,j}$
9: **end for**
10: Set $\underline{\mathrm{H}}_m = [h_{i,j}]_{i=1,...,m}^{j=1,...,m+1}$ and $V_m = [\mathbf{v}_1, ..., \mathbf{v}_m]$
11: **for** $k = 1$ to n_ω **do**
12:     Solve $\mathbb{C}^m \ni \mathbf{z}_k = \text{argmin}_\mathbf{z} \|(\underline{\mathrm{H}}_m - \tilde{\eta}_k\underline{\mathrm{I}}_m)\mathbf{z} - \|\mathbf{r}_0\|\mathbf{e}_1\|$ ▷ Shifts $\tilde{\eta}_k$ according to (11c)
13:     Resubstitute $\mathbf{y}_k = p_{n,k}(\mathcal{C})V_m\mathbf{z}_k$ ▷ Coefficients of $p_{n,k}$ according to (11a)-(11b)
14: **end for**

2.2.2   Inner-outer Krylov methods

We modify (7) by the substitutions, $\bar{\mathcal{K}} := \mathcal{K} - \omega_1\mathcal{M}$, $\bar{\mathcal{C}} := \bar{\mathcal{K}}\mathcal{P}(\tau)^{-1}$, and solve the equivalent systems,

$$(\bar{\mathcal{C}} - \bar{\eta}_k I)\mathbf{y}_k = \mathbf{b}, \quad \bar{\eta}_k := \frac{\omega_k - \omega_1}{\omega_k - \tau}, \quad k = 1, ..., n_\omega, \tag{12}$$

with the advantage that for $k = 1$ we solve the *base* system $\bar{\mathcal{C}}\mathbf{y}_1 = \mathbf{b}$ (unshifted). The nested multi-shift Krylov algorithm consists in general of m_i inner iterations and m_o outer iterations. The nested FOM-FGMRES algorithm [6] is a combination of inner multi-shift FOM (Algorithm 3) with outer flexible multi-shift GMRES (Algorithm 4). In [6] we derive that if the inner method yields collinear residuals in the sense,

$$\mathbf{r}_j^{(k)} = \gamma_j^{(k)}\mathbf{r}_j, \quad \gamma_j^{(k)} \in \mathbb{C} \text{ for } k = 1, ..., n_\omega, \tag{13}$$

for $\mathbf{r}_j$ being the residual of the base system after m_i inner iterations, we can preserve shift-invariance in the outer method. The consecutive collinearity factors of the inner method then appear on a diagonal matrix Γ_k of a modified Hessenberg matrix in the outer loop (see line 13 in Algorithm 4 and [6], respectively). More precisely, after m_o outer iterations, the solution to,

$$\mathbf{z}_k = \underset{\mathbf{z} \in \mathbb{C}^{m_o}}{\text{argmin}} \left\|\left((\underline{\mathrm{H}}_{m_o} - \underline{\mathrm{I}}_{m_o})\Gamma_k + \underline{\mathrm{I}}_{m_o}\right)\mathbf{y} - \|\mathbf{r}_0\|\mathbf{e}_1\right\|, \quad \mathbf{y}_k = Z_{m_o}^{(k)}\mathbf{z}_k, \tag{14}$$

yields approximate solutions to (12) in the search spaces $Z_{m_o}^{(k)}$ that minimize the 2-norm of the residual of the k-th shifted system, cf. [6]. In (14), the Hessenberg matrix $\underline{\mathrm{H}}_{m_o}$ corresponds to the base system, and $\Gamma_k := \text{diag}(\gamma_1^{(k)}, ..., \gamma_{m_o}^{(k)})$ is constructed from the collinearity factors in (13).

Algorithm 3 Inner multi-shift FOM for (12), cf. [17]

1: Set $\mathbf{r}_0 = \mathbf{b}$, $\mathbf{v}_1 = \mathbf{r}_0 / \|\mathbf{r}_0\|$ $\triangleright$ Initialization
2: **for** $j = 1$ to m_i **do**
3:     Apply $\mathbf{w} = \bar{\mathcal{K}}(\mathcal{K} - \tau\mathcal{M})^{-1}\mathbf{v}_j$ $\triangleright$ Apply matrix $\bar{\mathcal{C}}$, cf. definition in (12)
4:     **for** $i = 1$ to j **do** $\triangleright$ Arnoldi method
5:         $h_{i,j} = \mathbf{w}^{\mathsf{H}}\mathbf{v}_i$
6:         $\mathbf{w} = \mathbf{w} - h_{i,j}\mathbf{v}_i$
7:     **end for**
8:     Set $h_{j+1,j} = \|\mathbf{w}\|$ and $\mathbf{v}_{j+1} = \mathbf{w}/h_{j+1,j}$
9: **end for**
10: Set $H_{m_i} = [h_{i,j}]_{i=1,\dots,m_i}^{j=1,\dots,m_i}$ and $V_{m_i} = [\mathbf{v}_1, \dots, \mathbf{v}_{m_i}]$
11: **for** $k = 1$ to n_ω **do**
12:     Solve $\mathbb{C}^{m_i} \ni \mathbf{y}_k = (H_{m_i} - \bar{\eta}_k I_{m_i})^{-1}(\|\mathbf{r}_0\|\mathbf{e}_1)$ $\triangleright$ Shifted Hessenberg systems
13:     Compute $\gamma_k = \mathbf{y}_k(m_i)/\mathbf{y}_1(m_i)$ $\triangleright$ Collinearity factors relative to base system, cf. [6]
14:     Compute $\mathbf{x}_k = V_{m_i}\mathbf{y}_k$
15: **end for**

Algorithm 4 Outer multi-shift FGMRES for (12), cf. [6, 11]

1: Set $\mathbf{r}_0 = \mathbf{b}$, $\mathbf{v}_1 = \mathbf{r}_0 / \|\mathbf{r}_0\|$ $\triangleright$ Initialization
2: **for** $j = 1$ to m_o **do**
3:     $[\mathbf{z}_j^{(k)}, \{\gamma_j^{(k)}\}_{k=1}^{n_\omega}] = \texttt{msFOM}(\bar{\mathcal{C}}, \{\bar{\eta}_k\}_{k=1}^{n_\omega}, \mathbf{v}_j, \text{maxit}=m_i)$ $\triangleright$ Inner method (Algorithm 3)
4:     Apply $\mathbf{w} = \bar{\mathcal{K}}(\mathcal{K} - \tau\mathcal{M})^{-1}\mathbf{z}_j^{(k=1)}$ $\triangleright$ Apply matrix $\bar{\mathcal{C}}$ to base system
5:     **for** $i = 1$ to j **do** $\triangleright$ Arnoldi method
6:         $h_{i,j} = \mathbf{w}^{\mathsf{H}}\mathbf{v}_i$
7:         $\mathbf{w} = \mathbf{w} - h_{i,j}\mathbf{v}_i$
8:     **end for**
9:     Set $h_{j+1,j} = \|\mathbf{w}\|$ and $\mathbf{v}_{j+1} = \mathbf{w}/h_{j+1,j}$
10: **end for**
11: Set $\underline{H}_{m_o} = [h_{i,j}]_{i=1,\dots,m_o}^{j=1,\dots,m_o+1}$ and $Z_{m_o}^{(k)} = [\mathbf{z}_1^{(k)}, \dots, \mathbf{z}_{m_o}^{(k)}]$ $\triangleright$ Collect search spaces
12: **for** $k = 1$ to n_ω **do**
13:     Set $\underline{H}_{m_o}^{(k)} = (\underline{H}_{m_o} - \underline{I}_{m_o})\Gamma_k + \underline{I}_{m_o}$, where $\Gamma_k := \text{diag}(\gamma_1^{(k)}, \dots, \gamma_{m_o}^{(k)})$
14:     Solve $\mathbb{C}^{m_o} \ni \mathbf{y}_k = \text{argmin}_{\mathbf{y}} \|\underline{H}_{m_o}^{(k)}\mathbf{y} - \|\mathbf{r}_0\|\mathbf{e}_1\|$ $\triangleright$ Hessenberg systems as in (14)
15:     Compute $\mathbf{x}_k = Z_{m_o}^{(k)}\mathbf{y}_k$
16: **end for**

---

3   Numerical experiments

We focus our numerical experiments[1] on linear systems (1) that stem from a finite element [2, 5] discretization of the time-harmonic elastic wave equation [9]:

$$-\omega_k^2 \rho \mathbf{u}_k - \nabla\cdot\sigma(\mathbf{u}_k) = \mathbf{s}, \quad \mathbf{x} \in \Omega \subset \mathbb{R}^{d=\{2,3\}}, \tag{15a}$$

$$i\omega_k \rho \; B(c_p, c_s)\mathbf{u}_k + \sigma(\mathbf{u}_k)\hat{\mathbf{n}} = \mathbf{0}, \quad \mathbf{x} \in \partial\Omega_a, \tag{15b}$$

$$\sigma(\mathbf{u}_k)\hat{\mathbf{n}} = \mathbf{0}, \quad \mathbf{x} \in \partial\Omega_r. \tag{15c}$$

---

[1]For the finite element discretization we use the Python package `nutils` (http://nutils.org).

The Stress tensor in (15a) fulfills Hooke's law, $\sigma(\mathbf{u}_k) = \lambda(\mathbf{x})\left(\nabla\cdot\mathbf{u}_k\ I_d\right) + \mu(\mathbf{x})\left(\nabla\mathbf{u}_k + (\nabla\mathbf{u}_k)^\top\right)$, and we consider Sommerfeld radiation boundary conditions on $\partial\Omega_a$ that model absorption, and a free-surface boundary condition on $\partial\Omega_r$ (reflection). A finite element discretization with basis functions that are B-splines [8, Chapter 2] of degree $p \in \mathbb{N}_{>0}$ yields,

$$(K + i\omega_k C - \omega_k^2 M)\mathbf{u}_k = \mathbf{s}, \quad k = 1, ..., n_\omega, \tag{16}$$

where $\mathbf{u}_k$ contains FEM coefficients of the k-th displacement vector, and $\mathbf{s}$ models a source term. In the case of purely reflecting boundary conditions, $\partial\Omega_a = \emptyset$, we obtain $C = 0$; cf. [5]. The inhomogeneous set of parameters $\{\rho, c_p, c_s\}$ is described in Figure 1a. Here, we prescribe material-air boundary conditions at the upper boundary only, see Figure 1b.
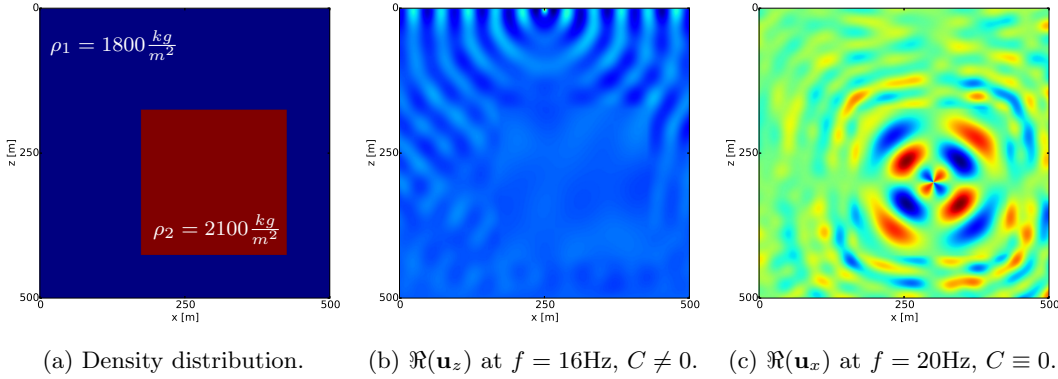

(a) Density distribution.   (b) $\Re(\mathbf{u}_z)$ at $f = 16$Hz, $C \neq 0$.   (c) $\Re(\mathbf{u}_x)$ at $f = 20$Hz, $C \equiv 0$.

Figure 1: Set-up of the 2D numerical experiments: Density distribution (left), and real part of z-component of the displacement at $f = 16$Hz (middle) and $f = 20$Hz (right). The speed of pressure waves and shear waves are $c_p = \{2000, 3000\}\frac{m}{s}$ and $c_s = \{800, 1600\}\frac{m}{s}$, respectively, and the Lamé parameters $\{\lambda, \mu\}$ in Hooke's law can be calculated accordingly.

When comparing convergence behavior of the matrix equation approach (2) with the shifted system re-formulation (3), we make use of the identity,

$$\|\mathbf{R}_m\|_\mathsf{F} = \sqrt{\sum_{k=1}^{n_\omega} \left\|\mathbf{r}_m^{(k)}\right\|_2^2}, \quad \text{for } \mathbf{R}_m := [\mathbf{r}_m^{(1)}, ..., \mathbf{r}_m^{(n_\omega)}] \in \mathbb{C}^{N \times n_\omega},$$

where $\left\{\mathbf{r}_m^{(k)}\right\}_{k=1}^{n_\omega}$ are the columns of $\mathbf{R}_m$ and *not* the residuals of the shifted systems. Since this way the block residual in Frobenius norm naturally is larger than an individual residual norm in 2-norm, we use the maximum 2-norm of the residuals of (3) as a *fair* stopping criteria. All numerical examples presented in this section have been implemented in `Python-3`, and executed on a computer with 4 CPUs `Intel I5` with 32 GB of RAM.

Experiment #1: Convergence study for viscous damping

As a first numerical experiment we consider the case when viscous damping is added to (16) via the substitution $\omega_k \mapsto (1 - \epsilon i)\omega_k$ for $\epsilon > 0$. As we explain in Section 2.2.1, the spectral radius of the polynomial preconditioner (8) can be minimized as a result of the optimal seed frequency described in [7]. Table 1 demonstrates that an increase of the polynomial degree n

reduces the number of iterations of Algorithm 2, cf. [10, 22]. The best CPU time is obtained for $n = 3$.

Table 1: Performance of Algorithm 2 for the case $C = 0$ and viscous damping parameter $\epsilon = 0.05$. We consider a fixed frequency range of $n_\omega = 5$ equally-spaced frequencies in $f_k \in [8, 16]$Hz, and $2 \times 200 \times 200$ `dofs`. The seed parameter τ is chosen *optimally* according to [7].

$n =$	10	5	4	3	2	1	0
# iterations	12	20	25	29	39	57	106
CPU time [s]	24.20	20.77	20.66	19.84	20.27	22.51	36.87

Table 2 compares the performance of the three algorithms when viscous damping is present, cf. Figure 1c. The shifted systems approaches outperform the matrix equation approach.

Table 2: Comparison of the three algorithms for the setup described in Table 1. The degree of the polynomial preconditioner is fixed at $n = 3$. We report CPU time in seconds and in parenthesis the number of iterations until `tol=1e-8`.

problem size	frequency range	n_ω	Gl-GMRES	poly-msGMRES	FOM-FGMRES
$2 \times 200 \times 200$	$\omega_k \in 2\pi[12, 16]$Hz	5	75.9 (125)	12.65 (12)	12.63 $(7 \cdot 8)$
$2 \times 200 \times 200$	$\omega_k \in 2\pi[10, 16]$Hz	5	183.1 (276)	15.31 (19)	16.04 $(12 \cdot 8)$
$2 \times 200 \times 200$	$\omega_k \in 2\pi[8, 16]$Hz	5	372.8 (540)	19.80 (29)	19.90 $(17 \cdot 8)$
$2 \times 200 \times 200$	$\omega_k \in 2\pi[12, 16]$Hz	15	195.5 (122)	15.71 (12)	13.41 $(7 \cdot 8)$
$2 \times 200 \times 200$	$\omega_k \in 2\pi[10, 16]$Hz	15	496.2 (267)	18.37 (19)	16.86 $(12 \cdot 8)$
$2 \times 200 \times 200$	$\omega_k \in 2\pi[8, 16]$Hz	15	1044.4 (522)	22.49 (29)	20.71 $(17 \cdot 8)$

Experiment #2: Suitability for wide frequency ranges

We next consider the undamped problem ($\epsilon = 0$) which is numerically more challenging. Here, we use $n = 0$ in Algorithm 2 because the spectral radius of the polynomial preconditioner is $R/|c| \equiv 1$, cf. [7, 21]. The experiments in Table 3 and 4 show that the matrix equation approach requires a large number of iterations, especially when the number of frequencies is increased. This is due to the fact that the union of the preconditioned spectrum needs to be well approximated by the global GMRES method.

Table 3: Comparison for undamped case and increased frequency range at a fixed seed parameter $\tau = (0.7 - 0.3i)\omega_{\max}$.

problem size	frequency range	n_ω	Gl-GMRES	poly-msGMRES	FOM-FGMRES
$2 \times 100 \times 100$	$\omega_k \in 2\pi[6, 8]$Hz	5	32.8 (125)	10.75 (96)	5.59 $(20 \cdot 8)$
$2 \times 100 \times 100$	$\omega_k \in 2\pi[4, 8]$Hz	5	64.7 (192)	10.81 (96)	5.55 $(20 \cdot 8)$
$2 \times 100 \times 100$	$\omega_k \in 2\pi[1, 8]$Hz	5	296.5 (934)	12.40 (106)	8.40 $(20 \cdot 11)$
$2 \times 100 \times 100$	$\omega_k \in 2\pi[6, 8]$Hz	15	51.9 (130)	11.63 (96)	6.06 $(20 \cdot 8)$
$2 \times 100 \times 100$	$\omega_k \in 2\pi[4, 8]$Hz	15	110.8 (237)	11.69 (96)	6.02 $(20 \cdot 8)$
$2 \times 100 \times 100$	$\omega_k \in 2\pi[1, 8]$Hz	15	601.7 (1199)	13.68 (106)	8.97 $(20 \cdot 11)$

Table 4: Setting as in Table 3 with $p = 2$ (quadratic splines).

problem size	frequency range	n_ω	G1-GMRES	poly-msGMRES	FOM-FGMRES
$2 \times 100 \times 100$	$\omega_k \in 2\pi[6,8]$Hz	15	103.7 (134)	18.68 (97)	13.93 $(20 \cdot 8)$
$2 \times 100 \times 100$	$\omega_k \in 2\pi[4,8]$Hz	15	208.4 (248)	19.59 (97)	13.96 $(20 \cdot 8)$
$2 \times 100 \times 100$	$\omega_k \in 2\pi[1,8]$Hz	15	1057.4 (1256)	28.87 (107)	18.95 $(20 \cdot 11)$

Experiment #3: Inexact solves for the shift-and-invert preconditioner

In Table 5 we exploit the use of an inexact LU factorization[2] for the shift-and-invert preconditioner in Algorithm 1. Therefore, we extend the test case in Figure 1a to 3D by an expansion in y-direction. The measured CPU times indicate the trade-off between decomposition time and overall number of iterations. In practice, more advanced inexact preconditioners such as multigrid [13, 14] or hierarchical matrix decompositions [5] are used in seismic applications.

Table 5: Inexact solves for the shift-and-invert preconditioner in Algorithm 1. We consider $n_\omega = 10$ equally-spaced frequencies with seed parameter $\tau = (0.7 - 0.3i)\omega_{\max}$. We use $\|\mathbf{R}_m\|_\mathsf{F} <$ 1e-8 as stopping criteria.

problem size	frequency range	preconditioner	setup time	CPU time	# iterations
$3 \times 35 \times 35 \times 35$	$\omega_k \in 2\pi[1,3]$Hz	exact inverse	4533.9	5396.2	53
$3 \times 35 \times 35 \times 35$	$\omega_k \in 2\pi[1,3]$Hz	iLU(10.0)	332.9	2852.3	482
$3 \times 35 \times 35 \times 35$	$\omega_k \in 2\pi[1,3]$Hz	iLU(20.0)	559.2	2179.0	367
$3 \times 35 \times 35 \times 35$	$\omega_k \in 2\pi[1,3]$Hz	iLU(30.0)	1061.4	2129.8	197

4   Conclusions

We have compared three GMRES-based algorithms for the simultaneous iterative solution of frequency-domain wave propagation problems at multiple frequencies that have the discretized form (1). The three approaches share that they require the application of a single shift-and-invert preconditioner at a so-called *seed* frequency. From our numerical experiments we draw the following conclusions:

- In the presence of viscous damping (Experiment #1) the optimal seed parameter derived in [7] implies a polynomial preconditioner (Algorithm 2) which, depending on the degree n of the polynomial, leads to a significant reduction of the (multi-shift) GMRES iterations. Without viscous damping, however, the spectral radius of the polynomial preconditioner equals one and no improvement has been observed.

- The matrix equation approach (Algorithm 1) builds up a block Krylov space that needs to approximate the union of all preconditioned spectra. This leads to a much larger number of overall iterations, and a worse performance compared with the shifted systems approach when a wide range of frequencies is considered. Because of the less restrictive framework, however, the shift-and-invert preconditioner (4) can be applied inexactly which leads to improvements especially for 3D problems (Experiment #3).

---

[2]We use python's built-in incomplete LU factorization `scipy.sparse.linalg.spilu`.

- For a wide frequency range (Experiment #2) we observe that the nested algorithm 3-4 outperforms the considered alternatives with respect to measured CPU time. This is due to short recurrence loops in the respective Arnoldi iterations. From Table 6 we note that the storage requirements for the flexible outer Krylov method can be limited when m_o is small compared to m_i.

Table 6: Comparison regarding memory requirements and costs-per-iteration when (1) has fixed problem size N and n_ω frequencies. Note that a single `MatVec` also requires a solve for the shift-and-invert preconditioner.

Algorithm	leading memory requirement	# `MatVec`'s
`Gl-GMRES(m)`	$N \cdot n_\omega \cdot m$ for $\mathbf{V}_m$ (in Alg. 1, line 10)	$n_\omega \cdot m$
`poly-msGMRES(m,n)`	$2N \cdot m$ for V_m (in Alg. 2, line 10)	$(n+1) \cdot m$
`FOM(m_i)-FGMRES(m_o)`	$2N \cdot n_\omega \cdot m_o$ for $Z_{m_o}^{(k)}$ (in Alg. 4, line 11)	$m_i \cdot m_o$

Acknowledgments

References

[1] M.I. Ahmad, D.B. Szyld, and M.B. van Gijzen. Preconditioned multishift BiCG for $\mathcal{H}_2$-optimal model reduction. Technical Report 12-06-15, Temple University, 2013.

[2] T. Airaksinen, A. Pennanen, and J. Toivanen. A damping preconditioner for time-harmonic wave equations in fluid and elastic material. *J. Comput. Phys.*, 228(5):1466:1479, 2009.

[3] R. Astudillo and M.B. van Gijzen. Induced Dimension Reduction Method for Solving Linear Matrix Equations. *Procedia Computer Science*, 80:222–232, 2016.

[4] T. Bakhos, P.K. Kitanidis, S. Ladenheim, A.K. Saibaba, and D.B. Szyld. Multipreconditioned GMRES for shifted systems. Technical Report 16-03-31, Department of Mathematics, Temple University, March 2016.

[5] M. Baumann, R. Astudillo, Y. Qiu, E. Ang, M.B. van Gijzen, and R.-E. Plessix. An MSSS-Preconditioned Matrix Equation Approach for the Time-Harmonic Elastic Wave Equation at Multiple Frequencies. Technical Report 16-04, Delft University of Technology, 2016.

[6] M. Baumann and M.B van Gijzen. Nested Krylov methods for shifted linear systems. *SIAM J. Sci. Comput.*, 37(5):S90–S112, 2015.

[7] M. Baumann and M.B. van Gijzen. An Efficient Two-level Preconditioner for Multi-Frequency Wave Propagation Problems. Technical Report 17-01, Delft University of Technology, 2017 (in preparation).

[8] J.A. Cottrell, T.J.R. Hughes, and Y. Bazilevs. *Isogeometric Analysis. Towards integration of CAD and FEA.* John Wiley & Son, Ltd., 2009.

[9] A.T. De Hoop. *Handbook of Radiation and Scattering of Waves.* Academic Press, London, United Kingdom, 1995.

[10] B. Fischer and R.W. Freund. On adaptive weighted polynomial preconditioning for Hermitian positive definite matrices. *SIAM J. Sci. Comput.*, 15:408–426, 1994.

[11] A. Frommer and U. Glässner. Restarted GMRES for Shifted Linear Systems. *SIAM J. Sci. Comput.*, 19(1):15–26, 1998.

[12] K. Jbilou, A. Messaoudi, and H. Sadok. Global FOM and GMRES algorithms for matrix equations. *Appl. Numer. Math.*, 31:49–63, 1999.

[13] C.D. Riyanti, Y.A. Erlangga, R.-E. Plessix, W.A. Mulder, C. Vuik, and C. Osterlee. A new iterative solver for the time-harmonic wave equation. *Geophysics*, 71(5):E57–E63, 2006.

[14] G. Rizzuti and W.A. Mulder. Multigrid-based 'shifted-Laplacian' preconditioning for the time-harmonic elastic wave equation. *Journal of Computational Physics*, 317:47–65, 2016.

[15] Y. Saad. *Iterative Methods for Sparse Linear Systems: Second Edition.* Society for Industrial and Applied Mathematics, 2003.

[16] A. Saibaba, T. Bakhos, and P. Kitanidis. A flexible Krylov solver for shifted systems with application to oscillatory hydraulic tomography. *SIAM J. Sci. Comput.*, 35(6):3001–3023, 2013.

[17] V. Simoncini. Restarted full orthogonalization method for shifted linear systems. *BIT Numerical Mathematics*, 43:459–466, 2003.

[18] V. Simoncini and F. Perotti. On the numerical solution of $(\lambda^2 A + \lambda B + C)x = b$ and application to structural dynamics. *SIAM J. Sci. Comput.*, 23:1875–1897, 2002.

[19] K.M. Soodhalter. Block Krylov Subspace Recycling for Shifted Systems with Unrelated Right-Hand Sides. *SIAM Journal on Scientific Computing*, 38(1):A302–A324, 2016.

[20] K.M. Soodhalter, D.B. Szyld, and F. Xue. Krylov subspace recycling for sequences of shifted linear systems. *Applied Numerical Mathematics*, 81C:105–118, 2014.

[21] M.B. van Gijzen, Y.A. Erlangga, and C. Vuik. Spectral Analysis of the Discrete Helmholtz Operator Preconditioned with a Shifted Laplacian. *SIAM J. Sci. Comput.*, 29(5):1942–1958, 2007.

[22] G. Wu, Y.-C. Wang, and X.-Q. Jin. A preconditioned and shifted GMRES algorithm for the Pagerank problem with multiple damping factors. *SIAM J. Sci. Comput.*, 34:2558–2575, 2012.

Code Availability

The source code of the implementations used to compute the presented numerical results can be obtained from:

`https://github.com/ManuelMBaumann/freqdom_compare`

and is authored by: Manuel Baumann and Martin B. van Gijzen.
Please contact Manuel Baumann for licensing information.